NANO LETTERS

Letter

pubs.acs.org/NanoLett

Dielectric Core–Shell Optical Antennas for Strong Solar Absorption Enhancement

Yiling Yu,[‡] Vivian E. Ferry,[§] A. Paul Alivisatos,[§] and Linyou Cao*[,†,‡]

[†]Department of Materials Science and Engineering and [‡]Department of Physics, North Carolina State University, Raleigh, North Carolina 27695, United States

[§]Department of Chemistry, University of California, Berkeley, and Materials Sciences Division, Lawrence Berkeley National Laboratory, Berkeley, California 94720, United States

Supporting Information

ABSTRACT: We demonstrate a new light trapping technique that exploits dielectric core–shell optical antennas to strongly enhance solar absorption. This approach can allow the thickness of active materials in solar cells lowered by almost 1 order of magnitude without scarifying solar absorption capability. For example, it can enable a 70 nm thick hydrogenated amorphous silicon (a-Si:H) thin film to absorb 90% of incident solar radiation above the bandgap, which would otherwise require a thickness of 400 nm in typical antireflective coated thin films. This strong enhancement arises from a controlled optical antenna effect in patterned core–shell nanostructures that consist of absorbing semiconductors and nonabsorbing dielectric materials. This core–shell optical antenna benefits from a multiplication of enhancements contributed by leaky mode resonances (LMRs) in the semiconductor part and antireflection effects in the dielectric part. We investigate the fundamental mechanism for this enhancement multiplication and demonstrate that the size ratio of the semiconductor and the dielectric parts in the core–shell structure is key for optimizing the enhancement. By enabling strong solar absorption enhancement, this approach holds promise for cost reduction and efficiency improvement of solar conversion devices, including solar cells and solar-to-fuel systems. It can generally apply to a wide range of inorganic and organic active materials. This dielectric core–shell antenna can also find applications in other photonic devices such as photodetectors, sensors, and solid-state lighting diodes.

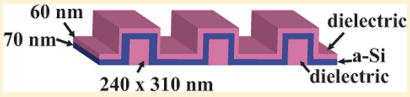

KEYWORDS: *Core–shell, optical antenna, nanowires, solar absorption, solar cells*

Solar radiation is by far the biggest source for clean, sustainable energy. However, its extensive utilization has been seriously delayed by the high cost and low efficiency of existing solar conversion devices.[1] Achieving cost reduction and efficiency improvement of these devices is necessary for the utilization of solar energy. Enhancing solar absorption by light trapping is one promising strategy to achieve this goal.[2] Enhancement in the solar absorption can relax the restrictions on the quality and quantity of active (absorbing) materials. In a high-performing solar cell, two constraints must be satisfied simultaneously: the active material must be optically thick so that every incident photon is used to generate electrons and holes, while the physical thickness should not be so large that these photogenerated carriers will recombine before being extracted. A typical way to satisfy these two constraints simultaneously is to make use of relatively pure, and therefore potentially expensive, materials for the absorber layer. By enabling more sunlight absorption in a reduced volume of material, light trapping offers an opportunity to circumvent this key limitation, opening up new options for low-cost fabrication of high-performance solar cells.[3]

Conventional wisdom for light trapping relies on textured surfaces and/or antireflection coatings (ARCs).[3−6] More recently, structures with subwavelength or wavelength dimensions have received considerable attention.[7−31] These structures rely upon resonant light–matter interactions[32,33] to concentrate sunlight in a confined volume that may greatly enhance the absorption of a semiconductor. A plethora of metallic nanostructures has been exploited for such absorption enhancement due to surface plasmon resonances (SPRs) of the metallic nanostructures.[17−23,25,28] Similarly, semiconductor nanostructures including nanoparticles, nanowires, nanopillars, and nanocones have also been demonstrated able to trap solar light and to enhance the absorption.[7−16,27,29] Here we present a different approach to trap and absorb solar light.

We demonstrate strong enhancements in the absorption of sunlight by exploiting a multiplication of enhancements in one-dimensional (1-D) core–shell nanostructures that consist of absorbing semiconductors and nonabsorbing dielectric materials, such as ZnO and Si_3N_4. 1-D semiconductor nanostructures have been previously shown to support leaky mode resonances (LMRs).[9,34,35] The nanostructures act as optical antennas that can effectively trap solar radiation to boost the absorption. In this work, we demonstrate that the optical antenna effect in 1-D nanostructures can be delicately engineered by constructing core–shell structures to further enhance the solar absorption. Fundamentally, this improvement is due to the combination of enhancements contributed by LMRs in the semiconductor and

Received: April 16, 2012
Revised: June 6, 2012
Published: June 11, 2012

antirefection effects of the dielectric of the core−shell structures. As a result, the key to optimizing the absorption enhancement is to design core−shell structures such that LMRs in the semiconductor part are well preserved and the dielectric layer acts as an effective ARC for solar radiation. Building upon this fundamental understanding, we propose a new design of optical antenna solar absorbers for practical applications in solar cells. With only 70 nm of thickness in the semiconductor (hydrogenated amorphous silicon, a-Si:H) layer, our designed structures can absorb 90% of all incident solar photons above the bandgap, comparable to the absorption in a 400 nm thick a-Si:H thin film enhanced by traditional ARCs. This core−shell optical antenna for efficient light trapping can generally apply to other semiconductors and organic materials.

Our studies start with single 1-D circular nanostructures, nanowires (NWs). Mathematical solutions to Maxwell's equations for circular cylinders are well-established.[36] This makes single 1-D circular nanostructures an ideal platform to explore fundamental physics underlying the absorption enhancement. Without losing generality, we focus on a-Si:H in this work and set the refractive index of the dielectric material at a constant of 2 across the whole solar spectrum, approximately consistent with real ZnO, ITO glass or Si_3N_4 materials.[37]

We define an integrated solar absorption J_{solar} as a figure of merit to evaluate the absorption capability of NWs for solar radiation. J_{solar} is defined as an integral of the spectral absorption efficiency $Q_{abs}(\lambda)$ of the NWs with the spectral photon flux density in the AM 1.5G solar spectrum $F_s(\lambda)$.[38]

$$J_{solar} = q \int F_s(\lambda) Q_{abs}(\lambda)\, d\lambda \quad (1)$$

where the absorption efficiency Q_{abs} is the normalized absorption cross-section C_{abs} with respect to geometrical cross-section C_{geo} ($Q_{abs} = C_{abs}/C_{geo}$) and is calculated with the well-established Lorentz−Mie formalism,[32] and q is the charge carried by one electron. J_{solar} bears a unit similar to short-circuit current density (mA/cm^2). But it should not be taken as a realistic value of the current density because the absorption cross section C_{abs} can be larger than the geometrical cross section C_{geo} of the structure. It is worthwhile noting that in the core−shell NWs only the semiconductor may absorb solar radiation, but in the calculation C_{geo} is the geometrical cross-section of the entire NW, including both semiconductor and dielectric components.

We have studied three different core−shell NWs, including semiconductor core/dielectric shells (referred as C−S1 NWs), dielectric core/semiconductor shells (referred as C−S2 NWs), and dielectric core/semiconductor layer/dielectric shells (referred as C−S3 NWs). In the calculations for the C−S1 and C−S3 NWs using eq 1, C_{geo} includes the geometrical cross-section of the nonabsorbing dielectric (semiconductor is inside of the dielectric), but for the C−S2 and the pure NWs, C_{geo} refers to the geometrical cross-section of the absorbing semiconductor (dielectric is embedded inside the semiconductor). To compare the solar absorption of semiconductor materials on a common ground, we define a weighted $J_{solar,w}$ by multiplying the calculated J_{solar} with the ratio between the geometrical cross section of the semiconductor part ($C_{geo,s}$) and the total geometrical cross section (C_{geo}), $J_{solar,w} = J_{solar}C_{geo}/C_{geo,s}$. Figure 1 shows the calculated $J_{solar,w}$ for core−shell NWs. The calculation of pure semiconductor NWs is also given as a reference. Significantly, we can find that the solar absorption

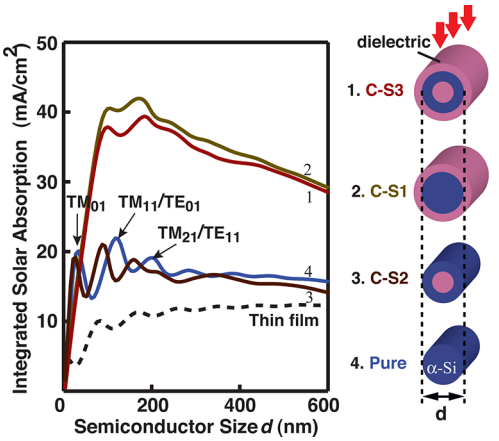

Figure 1. Calculated solar absorption of core−shell NWs that consist of absorbing semiconductor and nonabsorbing dielectric materials. The semiconductor is hydrogenated amorphous silicon (a-Si:H), and the refractive index of the dielectric is set to be a constant of 2 across the whole solar spectrum. The results shown are weighted $J_{solar,w}$. The weighted $J_{solar,w}$ is defined by multiplying integrated solar absorption J_{solar} with the ratio between the geometrical cross-section of the semiconductor part ($C_{geo,s}$) and the total geometrical cross-section (C_{geo}), $J_{solar,w} = J_{solar}C_{geo}/C_{geo,s}$. The peaks shown in the absorption are indicative of the contribution of LMRs. Typical leaky modes are labeled in the calculation for the single NW. The result for semiconductor (a-Si:H) thin films is also given as a reference (dashed black line). The red arrow to the upper right indicates the geometry of normal incidence used in the calculation.

can be enhanced twice as much by coating the structures with a layer of nonabsorbing dielectric materials, as indicated by curve 4 (pure NWs) versus curve 2 (C−S1 NWs) or curve 3 (C−S2) versus curve 1 (C−S3). We can also see that substituting a substantial amount of semiconductor NWs at the center with dielectric materials may only cause a very trivial decrease in the solar absorption, as shown by curve 3 (C−S2) versus curve 4 (pure) NWs or curve 2 (C−S1) vs curve 1 (C−S3). This indicates improved solar absorption per unit volume of semiconductor materials by the substitution.

To investigate the strong solar absorption enhancement in core−shell NWs, we examine the integrated solar absorption J_{solar} as a function of the physical dimensions of the NWs (Figures 2−3). For the semiconductor (core)−dielectric (shell) NW (C−S1), we find that a thickness of ∼70 nm in the dielectric shell always gives the largest J_{solar}. This optimized thickness (∼70 nm) varies little for cores of different semiconductor materials such as CdTe, GaAs, and $CuIn_xGa_{1-x}Se_2$ and shows a more or less linear dependence on the refractive index of the dielectric material (see Figure S1−S2 in the Supporting Information). This thickness dependence is similar to the behavior of traditional ARCs shown in Figure 2b (the refractive index of the ARC is set a constant of 2, the same as the dielectric in the core−shell NWs) and suggests that the dielectric shell of the C−S1 NWs acts as an ARC. The antireflection role of the dielectric shell can be further confirned from examining the absorption spectra. We can find that the dielectric shell of the C−S1 NWs gives rise to a broad absorption peak (Figure 2c,d). The wavelength λ_0 of the peak linearly depends on the thickness of the shell d_s, approximately following $n_s d_s = \lambda_0/4$, with n_s as the refractive index of the dielectric material (Figure 2c). For instance, the optimized thickness of 70 nm for this dielectric material (n_s =

dx.doi.org/10.1021/nl301435r | Nano Lett. 2012, 12, 3674−3681

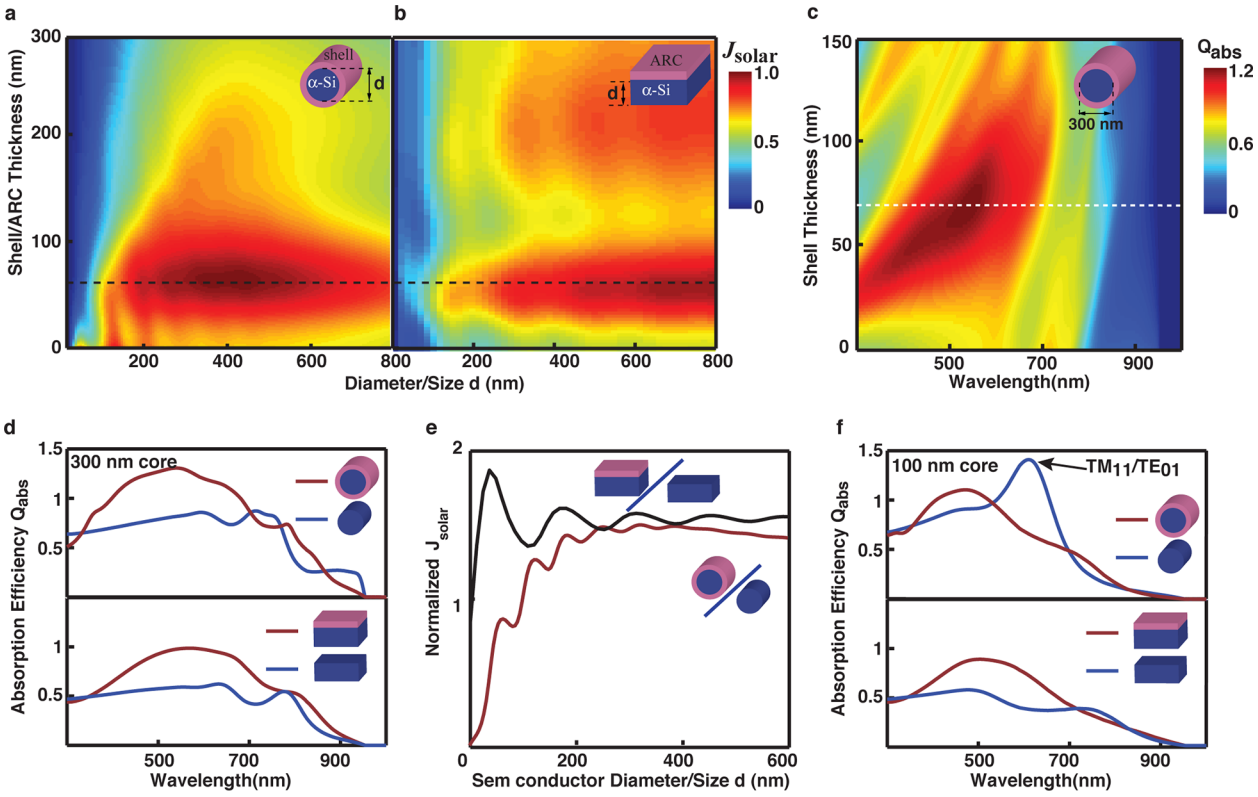

Figure 2. Solar absorption of standard core−shell structures (C−S1 NWs). (a) Two-dimensional plot of J_{solar} of core−shell NWs as functions of the diameter of the semiconductor core (horizontal axis) and the thickness of the dielectric shell (vertical axis). (b) Two-dimensional plot of J_{solar} of planar thin films as functions of the thickness of the semiconductor layer (horizontal axis) and the thickness of the ARC (vertical axis). The dashed black line indicates the optimized thickness in the dielectric layer for the solar absorption. For the convenience of comparison, the calculated J_{solar} in a and b are normalized to their maximum values, respectively. (c) Spectral absorption efficiency Q_{abs} of C−S1 NWs with a 300 nm diameter core as a function of the shell thickness (vertical axis). The dashed white line indicates the result replotted in d. (d, upper) Absorption spectra of a C−S1 NW with a 300 nm diameter core and a 70 nm thick dielectric shell (red curve) and of a pure 300 nm diameter semiconductor NW (blue curve); (lower) absorption spectra of planar semiconductor thin films in thickness of 300 nm with (red curve) and without (blue curve) a 70 nm thick ARC. (e) Normalized J_{solar} of C−S1 NWs with respect to pure semiconductor NWs in the same size as the core (red curve) and normalized J_{solar} of planar thin films enhanced by the traditional ARC with respect to bare planar thin films. (f, upper) Absorption spectra of a C−S1 NW with a 100 nm diameter core and a 70 nm thick shell (red curve) and a pure 100 nm diameter semiconductor NW (blue curve); the peak ~600 nm is from TM_{11}/TE_{01} as indicated. (f, lower) Absorption spectra of 100 nm thick planar semiconductor thin films with (red curve) and without (blue curve) a 70 nm thick ARC.

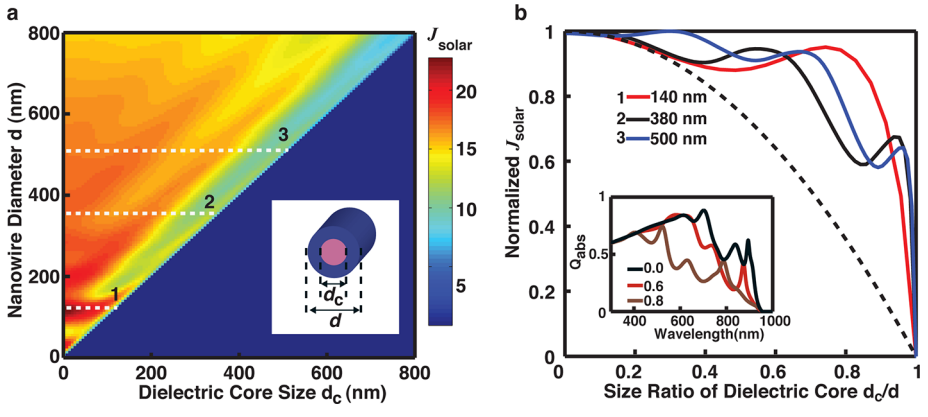

Figure 3. Solar absorption of inverse core−shell structures (C−S2 NWs). (a) Two-dimensional plot of J_{solar} of C−S2 NWs as functions of the diameter of the semiconductor part d (horizontal axis) and the diameter of the dielectric core d_c (vertical axis). The unit of the J_{solar} is mA/cm^2. The dashed white lines indicate the results replotted in b. Inset, schematic illustration of the inverse core−shell NW with the definitions for d and d_c indicated. (b) Normalized J_{solar} of C−S2 NWs as a function of the size ratio of the dielectric core d_c/d. The J_{solar} are normalized with respect to those of pure NWs in the same size as the C−S2 NWs. The dashed black line indicates the volume ratio of the semiconductor materials involved in the C−S2 NWs. Inset, absorption spectra of 380 nm diameter C−S2 NWs with different size ratios of the dielectric core.

dx.doi.org/10.1021/nl301435r | *Nano Lett.* 2012, 12, 3674−3681

2) gives an absorption peak at ~550 nm (Figure 2d, upper), matching the regime with the highest photon flux in the solar spectrum. Again, this linear dependence is consistent with the quarter-wave nature of traditional ARCs.[39]

In addition to the dependence on the dielectric shell, the J_{solar} of the C−S1 NW is also dependent on the size of the semiconductor core. For a dielectric shell with the optimized thickness (70 nm), a semiconductor core in the diameter of 300−500 nm gives the maximum J_{solar} (Figure 2a). To look in more detail, we normalize the J_{solar} of C−S1 NWs with the optimized shell (70 nm) with respect to that of pure NWs at the same size as the semiconductor core of the C−S1 NWs. As a reference, we perform similar normalization for ARC-coated semiconductor thin films (70 nm thick ARC) with respect to bare semiconductor thin films. This normalization is to elucidate how the role of the dielectric shell could change with the core size. Intuitively, besides from acting as an ARC as discussed in the preceding text, the dielectric shell may also perturb the intrinsic optical resonance (LMRs) in the semiconductor core as it changes the refractive index of the environment.[34,35] The balance of both effects would dictate the overall contribution of the dielectric shell to the solar absorption.

The normalized J_{solar} are plotted in Figure 2e as a function of the diameter of the semiconductor. We can see that the normalized J_{solar} of the C−S1 NWs rapidly increases with the size and approaches a constant of ~1.5 when the size is larger than 200 nm (red curve). The constant of ~1.5 is similar to the normalized J_{solar} of ARC-coated thin films (blue curve). This result suggests that, for a large semiconductor core (>200 nm), the 70 nm thick dielectric shell primarily acts as an ARC, without substantially perturbing the intrinsic optical resonances (LMRs) in the core NW. However, the 70 nm thick dielectric shell may perturb the intrinsic LMRs in the core when the core is smaller than 200 nm. To confirm, we examine the absorption spectra of typical NWs with and without the dielectric coating. We can find that, for a 300 nm diameter semiconductor core, the dielectric shell gives a broad absorption peak around ~550 nm with trivial changes at the other wavelengths (Figure 2d, upper panel), similar to traditional ARCs for thin films (Figure 2d, lower panel). However, for a 100 nm core, it suppresses the absorption for some wavelengths (~600 nm) that can be strongly absorbed in a pure NW. As a result, we believe that the maximum J_{solar} appearing at the core size of 350−500 nm (Figure 2a) is due to the integration of enhancements from LMRs in the semiconductor core and antireflection effects of the dielectric shell.

Unlike the semiconductor (core)−dielectric(shell) structure (C−S1 NWs), the inverse structure (C−S2 NWs) typically does not provide greater J_{solar} than pure NWs but may generate a comparable value with a reduced volume of semiconductor materials. We consider the inverse core−shell structure as a semiconductor NW with the central part substituted by nonabsorbing dielectric materials and plot the calculated J_{solar} as a function of the size of the whole NW d and the size of the dielectric core d_c (Figure 3a). The J_{solar} of the C−S2 NW can be found to generally decrease with increasing d_c. To better understand this size dependence, we normalize the J_{solar} of the C−S2 NW with respect to that of a pure NW in a size of d and plot the normalized J_{solar} as a function of the size ratio of the dielectric core (d_c/d) in Figure 3b. The volume ratio $(1 - (d_c/d)^2)$ of the semiconductor material in the C−S2 NW is also plotted (the dashed black line) to illustrate that the J_{solar} does not scale with the volume of the absorbing material involved. We can see that the J_{solar} of the C−S2 NWs always show a slow decrease with the size ratio d_c/d increasing and only quickly drop when the ratio increases up to 0.7 or higher (Figure 3b). Corroborating evidence can be seen in the spectral absorption of a typical C−S2 NW (380 nm diameter) that shows the absorption indeed does not decrease much until the ratio d_c/d is up to 0.8 (Figure 3b, inset). These results suggests that the intrinsic optical resonance in the semiconductor NW may not be substantially interrupted by the substitution of a dielectric core until the core becomes a very substantial part of the NW.

To fundamentally understand the solar absorption enhancement in the core−shell NWs, we study leaky modes of these NWs with a particular focus on the dependence of the modes on physical dimensions. Leaky modes have been previously demonstrated to dominate the light absorption of 1-D semiconductor nanostructures.[9,34,35] Knowledge of the leaky modes is expected to provide better understanding, prediction, and guidance for the optimization of the solar absorption.

As illustrated in Figure 4, we arbitrarily set the refractive indices of the core, the shell, and the environment as n_2, n_1, and

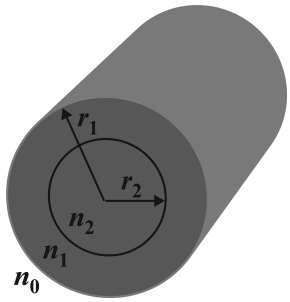

Figure 4. Schematic illustration of core−shell NWs for the analysis of leaky modes. The radii of the core and the shell are assigned as r_2 and r_1, respectively. The refractive indexes of the environment, the shell, and the core are assigned as n_0, n_1, and n_2, respectively.

n_0 and the radii of the core and the whole NW as r_2 and r_1, respectively. For simplicity, here we only study transverse magnetic (TM) leaky modes that are defined with electric fields parallel to the NW axis (the results for other leaky modes such as transverse electric (TE) modes are similar to the TM modes). By solving Maxwell's equations in cylindrical coordinate and matching boundary conditions at the core−shell and the shell−environment interfaces, we can derive the TM leaky modes of the core−shell structure from a matrix as follows:

$$\det\begin{bmatrix} J_m(n_2kr_2) & -J_m(n_1kr_2) & -H_m(n_1kr_2) & 0 \\ 0 & J_m(n_1kr_1) & H_m(n_1kr_1) & -H_m(n_0kr_1) \\ n_2J_m'(n_2kr_2) & -n_1J_m(n_1kr_2) & -n_1H_m(n_1kr_2) & 0 \\ 0 & n_1J_m(n_1kr_1) & n_1H_m(n_1kr_1) & -n_0H_m'(n_0kr_1) \end{bmatrix} = 0 \quad (2)$$

where k is the wavevector in free space, J_m and H_m are the mth order Bessel function of the first kind and Hankel function of the first kind, and the prime denotes differentiation with respect to related arguments. For simplicity, we set the refractive index of the semiconductor to a frequency-independent constant of 4, which is a reasonable approximation for typical semiconductor materials (the imaginary part of the refractive index of the

dx.doi.org/10.1021/nl301435r | Nano Lett. 2012, 12, 3674−3681

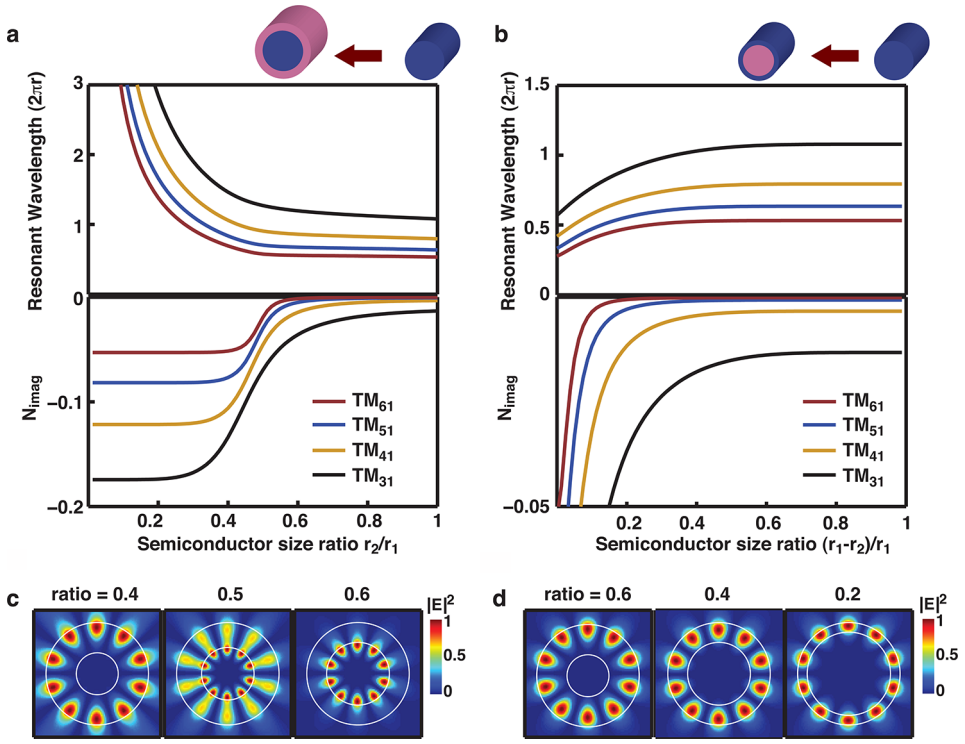

Figure 5. Dependence of leaky modes on the physical dimension of core−shell nanostructures. (a) The resonant wavelength (upper) and the imaginary eigenvalue N_{imag} (lower) of typical leaky modes in the standard core−shell structure (C−S1 NWs) as a function of the size ratio of the semiconductor core r_2/r_1. (b) Resonant wavelength (upper) and the N_{imag} (lower) of typical leaky modes in the reverse core−shell structure (C−S2 NWs) as functions of the size ratio of the semiconductor shell $(r_1 - r_2)/r_1$. (c) Electric field distributions of a typical leaky mode (TM_{51}) in the C−S1 NWs with different size ratios of the semiconductor core. (d) Electric field distributions of a typical leaky mode (TM_{51}) in the C−S2 NWs with different size ratios of the semiconductor shell.

semiconductor is generally small and can be ignored without substantially changing the result). The refractive index of the dielectric material is set to be 2 as in the preceding discussion. Numerical implementation of eq 2 gives complex solutions for a normalized parameter kr_1, $kr_1 = N_{real} + iN_{imag}$. Each complex solution is the eigenvalue of a specific leaky mode. Leaky modes can be characterized by an azimuthal mode number, m, which indicates an effective number of wavelengths around the wire circumference and a radial order number, l, describing the number of radial field maxima within the cylinder (for example, TM_{ml}).[34] The real part (N_{real}) of the eigenvalue is related with the wavelength where the optical resonance (LMRs) takes place ($\lambda = 2\pi r_1/N_{real}$), and the imaginary part (N_{imag}) dictates the spectral width of the optical resonance. Typically, the resonant wavelength λ and the width of the resonant peak determine the absorption contributed by each leaky mode.[35] For this reason, we focus on studying how the resonant wavelength λ and the imaginary eigenvalue N_{imag} of leaky modes evolve with the physical dimensions of core−shell structures.

Figure 5 shows calculations for typical leaky modes in both of the core−shell structures. The results are plotted as a function of the size ratio of the semiconductor, which is r_2/r_1 for the C−S1 semiconductor (core)−dielectric (shell) structure and $(r_1 - r_2)/r_1$ for the C−S2 following the schematic illustration given in Figure 4. We find that the ratio of 0.5 emerges as a tipping point for the leaky modes in the C−S1 NWs. The resonant wavelength λ of a given leaky mode remains largely constant for ratios larger than 0.5 and rapidly increases (red shift) for smaller ratios. Additionally, the N_{imag} sees a rapid transition at the regime close to the ratio of 0.5 and remains virtually independent before and after the transition. This tipping point of 0.5 can be better understood through examining the electric field distribution of leaky modes. Figure 5c shows the electric field distribution for a typical mode, TM_{51}. The electric field can be found concentrated in the core for a ratio >0.6, in the dielectric shell layer for a ratio <0.4, and distributed in both core and shell layers for a ratio in between. Ideal solar absorption requires the optical field to be concentrated in the semiconductor layer. As a result, for a dielectric shell with the optimized thickness of 70 nm, the core should be larger than 210 nm in diameter (the core ratio >0.6) for optimized solar absorption. In this case, leaky modes (such as the resonant wavelength λ and the N_{imag}) of the semiconductor core are left largely intact by the dielectric shell. This is consistent with the results shown in Figure 2, which indicates that, for semiconductor cores larger than 200 nm, the 70 nm thick dielectric shell primarily acts as an ARC without strongly perturbing the intrinsic optical resonances in the core.

The leaky modes in the C−S2 dielectric (core)−semiconductor (shell) structure also show a strong dependence on the size ratio. Similarly, the resonant wavelength λ and the N_{imag} of these leaky modes remain constant for large semiconductor ratios, but subject to substantial changes when the ratio drops below a certain tipping point. This tipping point varies with different leaky modes and is typically larger than 0.5. For instance, it is around 0.6 for the TM_{51} mode. This tipping point can also be understood from the electric field distribution (Figure 5d). We can find that the electric field tends to be concentrated in the region close to the outmost edge of the

dx.doi.org/10.1021/nl301435r | Nano Lett. 2012, 12, 3674−3681

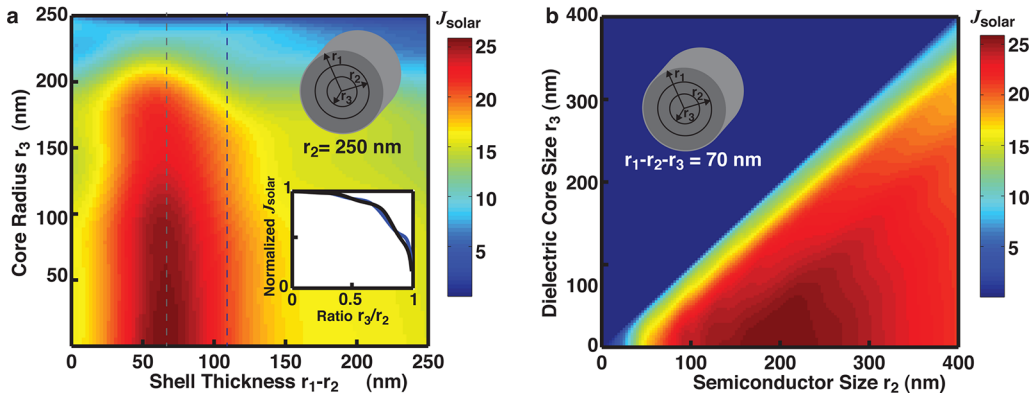

Figure 6. Solar absorption in combined core−shell structures (C−S3 NWs). (a) Two-dimensional plot of J_{solar} of the C−S3 NWs as functions of the thickness of the outer dielectric shell $r_1-r_2-r_3$ (horizontal axis) and the radius of the inner dielectric core r_3 (vertical axis). The unit of the J_{solar} is mA/cm^2. The radius of the intermediate semiconductor layer is fixed as r_2 = 250 nm. The dashed lines indicate the results replotted in the inset: (upper) schematics illustration of the core-two-shell structures; (lower) normalized J_{solar} as a function of the size ratio of the dielectric core r_3/r_2. The J_{solar} is normalized with respect to those of standard core−shell NWs without the dielectric inner core (r_3 = 0). (b) Two-dimensional plot of J_{solar} of the C−S3 NWs as functions of the radius of the semiconductor layer r_2 (horizontal axis) and the radius of the inner dielectric core r_3 (vertical axis). The thickness of the outer dielectric shell is fixed as $r_1-r_2-r_3$ = 70 nm.

NW. Therefore, substituting part of the semiconductor NW at the center with dielectric materials may not touch and affect the field distribution unless the substitution is substantial (the size ratio of the semiconductor layer <0.5). This matches the results given in Figure 3 that the J_{solar} of the C−S2 NW slowly decreases with the dielectric size increasing until the dielectric core becomes a substantial part of the NW.

This correlation between leaky modes and physical features can apply to more complex structures, such as dielectric core/semiconductor layer/dielectric shell (C−S3) NWs. Figure 6 shows calculated J_{solar} for the C−S3 NWs as functions of r_1, r_2, and r_3 (r_1, r_2, and r_3 are the radii of the NW, the semiconductor layer, and the inner core as illustrated in Figure 6 inset). The C−S3 NW can be found responding to sunlight just as a simple combination of a C−S1 and a C−S2 structures. For a given size in the semiconductor part (r_2), a thickness of 70 nm in the outer dielectric shell provides an optimized J_{SC} (Figure 6a). For an optimized dielectric shell, a semiconductor in radius of around 150−250 nm (r_2) gives the maximum J_{solar} (Figure 6b). Additionally, the J_{solar} of the C−S3 NW depends on the ratio of the radius of the semiconductor layers (r_2) and that of the inner dielectric core (r_s) in a way similar to the J_{solar} of the C−S2 structure. The normalized J_{solar} of the C−S3 NW slowly decreases with the ratio of the dielectric core (r_3/r_2) increasing (Figure 6a inset and b). This result indicates that the understanding of basic core−shell structures (C−S1 and C−S2) can serve a useful guideline for the rational designs of more complex structures with optimized absorption enhancements.

The fundamental understanding that we have developed from the studies of single core−shell NWs can be a very useful reference for the rational design of large-scale solar absorbing structures. Our previous work demonstrated that the optical resonances in each individual NWs of an array should be largely preserved to achieve optimized solar absorption.[9] To illustrate this notion, we herein demonstrate a design of an array of core-two-shell NWs similar to the C−S3 NWs. We use rectangular NWs instead of circular ones as building blocks for the array. Our previous research has demonstrated that all 1-D semiconductor nanostructures show similar solar absorption properties regardless the cross-sectional shape, such as circular, rectangular, triangular, and hexagonal.[9] An array of rectangular NWs can be readily fabricated using standard, scalable thin film deposition and patterning techniques, which is very important for practical applications.

From the discussion of Figure 6, we learn that a core-two-shell structure may have optimized absorption with a dielectric shell in thickness of ∼55−70 nm (Figure 6a) and a semiconductor layer (r_2) in radii of ∼150−250 nm (Figure 6b). Following this guidance, we design an array of core-two-shell NWs as illustrated in Figure 7a. For the ease of fabrication,

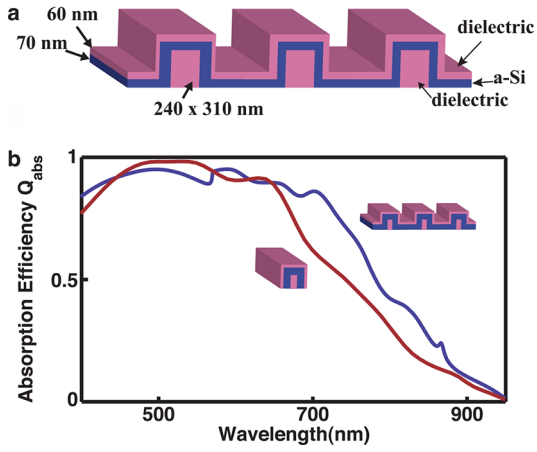

Figure 7. Design of large-scale arrays of core−shell NWs for practical applications. (a) Schematic illustration of the proposed design, the outer dielectric coating in thickness of 60 nm, the intermediate semiconductor layer in thickness of 70 nm, and the inner dielectric core in width of 240 nm and in height of 310 nm. (b) Spectral absorption efficiency of the NW array (red curve) and a standing-alone NW building block (blue curve). The absorption of the standing-alone block is scaled by a constant of 0.8 for visual convenience.

the NW is designed to have a quasi-core−shell structure that consists of conformal coatings of semiconductor and dielectric materials on predefined 1-D dielectric nanostrutures. Without substantial efforts in structure optimization, the thicknesses of the outer dielectric coating and the semiconductor layer are set at 60 nm and 70 nm, respectively; the inner core is 240 nm in width and 310 nm in height. The period of the array is set to be

dx.doi.org/10.1021/nl301435r | Nano Lett. 2012, 12, 3674−3681

570 nm, which is designed to preserve the optical resonances in each individual NWs. To keep the discussion as general as possible, we assume no substrate underneath the NW array. Our full-field finite-difference time-domain (FDTD) simulations show that this proposed NW array can strongly absorb sunlight. Using a-Si:H as an example, with a thickness of only 70 nm in the semiconductor layer, it can provide a J_{SC} of 20.3 mA/cm^2, accounting for 90% of all solar photons above the bandgap of a-Si:H (22.5 mA/cm^2, a-Si:H bandgap is 1.7 eV).[38] It is worthwhile to note that adding a semi-infinite silica substrate underneath the array shows a very negligible effect on the solar absorption. As a reference, to absorb a similar amount of sunlight using conventional ARC-coated a-Si:H thin films requires a thickness of 400 nm in the semiconductor (see Figure S3 in the Supporting Information). We find that the strong, broad absorption of the array is very similar to that of single NWs, which indicates that the optical resonances in individual NWs indeed play a dominant role in enhancing the solar absorption of the array.

In conclusion, our studies demonstrate that core−shell nanostructures that consist of absorbing semiconductor and nonabsorbing dielectric materials stand as a highly effective platform for enhancing solar absorption. The extraordinary absorption enhancement of the core−shell structure is due to a multiplication of contributions from LMRs in the semiconductor part and antireflection effects in the dielectric part. Key to optimizing the absorption enhancement is to preserve the LMRs in the semiconductor part and to make the dielectric part an effective ARC for solar radiation. As a general design principle, the thickness of the dielectric shell should be optimized for the antireflection of solar radiation, and the size ratio of the semiconductor core in the semiconductor (core)−dielectric (shell) structure needs to be larger than 0.5−0.6 to preserve the intrinsic LMRs. While focusing on a-Si:H in this work, this technique of dielectric core−shell optical antennas can generally apply to all other absorbing materials, such as other semiconductors and organic materials. The structure with a quasi-core−shell configuration as shown in Figure 7a can be easily fabricated with standard, scalable thin film deposition and patterning technologies. In addition to the great promise for solar energy, this technique may also find applications in other photonic devices, including photodetectors, sensors, and solid-state lighting diodes.

■ ASSOCIATED CONTENT

Supporting Information

Two-dimensional plots of calculated J_{solar} for standard core-shell NWs (C-S1 NWs) as functions of the diameter of the semiconductor core and the thickness of the dielectric shell (Figure S1) and as functions of the thickness and the refractive index of the dielectric shell (Figure S2); calculated J_{solar} for a-Si thin films and a-Si thin films enhanced by traditional ARCs as a function of the film thickness (Figure S3). This material is available free of charge via the Internet at http://pubs.acs.org.

■ AUTHOR INFORMATION

Corresponding Author

*E-mail: lcao2@ncsu.edu.

Notes

The authors declare no competing financial interest.

■ ACKNOWLEDGMENTS

Y.Y. and L.C. acknowledge useful discussions with Xiang Ji. L.C. acknowledges North Carolina State University start-up fund and the Miller Institute at the University of California for financial support. Part of work on the simulation of solar absorption in single core−shell nanowires was supported by the "Light-Material Interactions in Energy Conversion" Energy Frontiers Research Center, United States Department of Energy, under Grant No. DE-SC0001293.

■ REFERENCES

(1) Lewis, N. S. *Science* **2007**, *315*, 798.
(2) *Basic Research Needs for Solar Energy Utilization*; U.S. Department of Energy, Washington, DC, 2005.
(3) Nelson, J. *Physics of Solar Cell*; Imperial College Press: London, 2008.
(4) Kuo, M.-L.; Poxson, D. J.; Kim, Y. S.; Mont, F. W.; Kim, J. K.; Schubert, E. F.; Lin, S.-Y. *Opt. Lett.* **2008**, *33*, 2527.
(5) Rim, S.; Zhao, S.; Scully, S. R.; McGehee, M. D.; Peumans, P. *Appl. Phys. Lett.* **2007**, *91*, 243501.
(6) Zhao, J.; Green, M. A. *IEEE Trans. Electron Devices* **1991**, *38*, 1925.
(7) Bandiera, S.; Jacob, D.; Muller, T.; Marquier, F.; Laroche, M.; Greffet, J. J. *Appl. Phys. Lett.* **2008**, *93*, 193103.
(8) Bao, H.; Ruan, X. *Opt. Express* **2010**, *35*, 3378.
(9) Cao, L.; Fan, P.; Vasedev, A.; White, J. S.; Yu, Z.; Cai, W.; Schuller, J. A.; Fan, S.; Brongersma, M. L. *Nano Lett.* **2010**, *10*, 439.
(10) Fan, Z.; Kapadia, R.; Leu, P. W.; Zhang, X.; Chueh, Y.; Takei, K.; Yu, K.; Jamshidi, A.; Rathore, A. A.; Ruebusch, D. J.; Wu, M.; Javey, A. *Nano Lett.* **2010**, *10*, 3823.
(11) Garnett, E.; Yang, P. *Nano Lett.* **2010**, *10*, 1082.
(12) Kelzenberg, M. D.; Boettcher, S. W.; Pethkiewicz, J. A.; Turner-Evans, D. B.; Putnam, M. C.; Warren, E. L.; Spurgeon, J. M.; Briggs, R. M.; Lewis, N. S.; Atwater, H. A. *Nat. Mater.* **2010**, *9*, 239.
(13) Lin, C.; Povinelli, M. L. *Opt. Express* **2009**, *17*, 19371−.
(14) Liu, W. F.; Oh, J. I.; Shen, W. Z. *Nanotechnology* **2011**, *22*, 125705.
(15) Street, R. A.; Wong, W. S.; Paulson, C. *Nano Lett.* **2009**, *9*, 3494.
(16) Zhu, J.; Yu, Z.; Burkard, G. F.; Hsu, C. M.; Connor, S. T.; Xu, Y.; Wang, Q.; McGehee, M.; Fan, S.; Cui, Y. *Nano Lett.* **2009**, *9*, 279.
(17) Catchpole, K. R.; Polman, A. *Opt. Express* **2008**, *16*, 21793.
(18) Ferry, V. E.; Sweatlock, L. A.; Pacifici, D.; Atwater, H. A. *Nano Lett.* **2008**, *8*, 4391.
(19) Pala, R. A.; White, J. S.; Barnard, E.; Liu, J.; Brongersma, M. L. *Adv. Mater.* **2009**, *21*, 1.
(20) Schuller, J. A.; Barnard, E. S.; Cai, W.; Jun, Y. C.; White, J. S.; Brongersma, M. L. *Nat. Mater.* **2010**, *9*, 193.
(21) Atwater, H. A.; Polman, A. *Nat. Mater.* **2009**, *9*, 205.
(22) Pillai, S.; Catchpole, K. R.; Truke, T.; Green, M. A. *J. Appl. Phys.* **2007**, *101*, 093105.
(23) Lindquist, N. C.; Luhman, W. A.; Oh, S. H.; Holmes, R. J. *Appl. Phys. Lett.* **2008**, *93*, 123308.
(24) Hu, L.; Chen, G. *Nano Lett.* **2007**, *7*, 3249.
(25) Munday, J. N.; Atwater, H. A. *Nano Lett.* **2011**, *11*, 2195.
(26) Grandidier, J.; Callahan, D. M.; Munday, J. N.; Atwater, H. A. *Adv. Mater.* **2011**, *23*, 1272.
(27) Fan, Z.; Razavi, H.; Do, J.; Moriwaki, A.; Ergen, O.; Chueh, Y.; Leu, P. W.; Ho, J. C.; Takahashi, T.; Reichertz, L. A.; Neale, S.; Yu, K.; Wu, M.; Ager, J. W.; Javey, A. *Nat. Mater.* **2009**, *8*, 648.
(28) Ferry, V. E.; Polman, A.; Atwater, H. A. *ACS Nano* **2011**, *11*, 10055.
(29) Mann, S. A.; Grotic, R. R., Jr.; Osgood, R. M.; Schuller, J. A. *Opt. Express* **2011**, *19*, 25729.
(30) Kuang, Y.; Werf, K. H. M. v. d.; Houweling, Z. S.; Schropp, R. E. *Appl. Phys. Lett.* **2011**, *98*, 113111.
(31) Naughton, M. J.; Kempa, K.; Ren, Z. F.; Gao, Y.; Rybczynski, J.; Argenti, N.; Gao, W.; Wang, Y.; Peng, Y.; Naughton, J. R.; McMahon,

G.; Paudel, T.; Lan, Y. C.; Burns, M. J.; Shepard, A.; Clary, M.; Ballif, C.; Huang, F.-J.; Soderstrom, T.; Cuberto, O.; Eminian, C. *Phys. Status Solidi* **2010**, *7*, 181.
(32) Bohren, C. F.; Huffman, D. R. *Absorption and Scattering of Light by Small Particles*; John Wiley & Sons, Inc.: New York, 1998.
(33) Kreibig, U.; Vollmer, M. *Optical Properties of Metal Clusters*; Springer: Berlin, 1995.
(34) Cao, L.; White, J. S.; Park, J. S.; Clemens, B. M.; Schuller, J. A.; Brongersma, M. L. *Nat. Mater.* **2009**, *8*, 643.
(35) Yu, Y.; Cao, L. *Opt. Express* **2012**, *13*, 13847.
(36) Kong, J. A. *Electromagnetic Wave Theory*; John Wiley & Sons: New York, 1985.
(37) Palik, E. D. *Handbook of Optical Constants of Solids*; Acadamic Press: London, 1985.
(38) ASTM G-173-03. *Terrestrial Reference Spectra for Photovoltaic Performance Evaluation*; American Society for Testing Materials International: West Conshohocken, PA, 2008.
(39) Inan, U. S.; Inan, A. S. *Electromagnetic Waves*; Prentice Hall: Upper Saddle River, NJ, 2000.

dx.doi.org/10.1021/nl301435r | *Nano Lett.* 2012, 12, 3674−3681